Reliability Assessment of Transformerless PV Inverters Considering Mission Profiles

Yang, Yongheng; Wang, Huai; Blaabjerg, Frede

Published in:
International Journal of Photoenergy

DOI (link to publication from Publisher):
10.1155/2015/968269

Publication date:
2015

Document Version
Early version, also known as pre-print

Research Article (Invited)

Reliability Assessment of Transformerless PV Inverters Considering Mission Profiles

Yongheng Yang, Huai Wang, and Frede Blaabjerg

Department of Energy Technology, Aalborg University, Pontoppidanstraede 101, Aalborg DK-9220, Denmark

Correspondence should be addressed to Yongheng Yang: yoy@et.aau.dk

Manuscript submitted on November 17, 2014; revised on January 26, 2015; accepted on February 9, 2015

Abstract- Due to the small volume and high efficiency, transformerless inverters have gained much popularity in grid-connected PV applications, where minimizing leakage current injection is mandatory. This can be achieved either by modifying the modulation schemes or adding extra power switching devices, resulting in an uneven distribution of the power losses on the switching devices. Consequently, the device thermal loading is redistributed, and thus may alter the entire inverter reliability performance, especially under a long-term operation. In this consideration, this paper assesses the device reliability of three transformerless inverters under a yearly mission profile (i.e., solar irradiance and ambient temperature). The mission profile is translated to device thermal loading, which is used for lifetime prediction. Comparison results reveal the lifetime mismatches among the power switching devices operating under the same condition, which offers new thoughts for a robust design and a reliable operation of grid-connected transformerless PV inverters with high efficiency.

1. Introduction

Power electronics converter technology has enabled more and more renewable energy installations in recent years, which is also associated with an increasing demand for higher efficiency and higher reliability [1]-[7]. In order to reduce the cost of energy, the demand will be further strengthened in the future energy mix dominated by wind turbine systems and Photo-Voltaic (PV) systems [8]-[11]. Transformerless PV inverters have gained much reputation in the European market in terms of high efficiency, small size, and low weight compared to their counterparts [7], [12]-[16]. Its popularity and its magnificence in conversion efficiency induce a shift in inverter technology in the United States recently [18]. Therefore, an even wide-scale adoption of transformerless PV inverters in the future grid-friendly systems is predictable.

Till now, a vast of transformerless PV inverters have been developed [13]-[21], and many of those topologies have been successfully commercialized in residential PV applications, where size and efficiency are the main concerns. However, "transformerless" is also required to minimize the leakage current injections for safety due to the removal of the galvanic isolation. This is typically achieved by either developing a special suitable modulation scheme or adding extra power switching devices [21]. For instance, in [19] and [20], optimization approaches have been proposed to improve the performance of transformerless PV inverters, while in [12]-[14], additional power switching devices have been introduced to the traditional full-bridge PV inverter. However, such software or hardware modifications will alter the power loss distributions on the power switching devices, thus contributing to uneven thermal loading in the PV inverters.

Due to the intermittency of solar energy, transformerless PV inverters have to handle with a fluctuating power. Thus, the thermal loading on each power switching device will be different under a long-term mission profile (e.g., a yearly solar irradiance and ambient temperature profile) [22]-[25]. The varying thermal loading (appears as fluctuating junction temperature) of the power switching devices is one of the main failure contributors for the power electronics devices [23]-[30]. As a consequence, the thermal stress difference among the power switching devices will possibly make the entire transformerless PV inverter fail to operate [26]-[33]. Although more advanced transformerless inverters with a main focus on efficiency are coming on market, there is still a lack of a reliability-oriented investigation considering mission profiles for those PV inverters. However, such an investigation allows new thoughts for a robust design and a reliable operation of PV system. As a result, a reduction of the cost of can be attained since both the efficiency and the reliability of transformerless PV inverters are enhanced.

Taking the above into consideration, this paper explores the thermal performance of three selected transformerless PV inverters under a yearly mission profile, which thus allows a qualitative reliability assessment of the PV inverters beyond efficiency achievements. Firstly, a description of the selected transformerless PV topologies is presented in § 2. Focus has been put on the mission profile translation to the corresponding device thermal loading of the transformerless inverters in § 3, where a mission profile based reliability evaluation approach is also introduced. In accordance with the translated thermal loading profiles, § 4 thus conducts an assessment of the device reliability in those PV inverters before the conclusions.

2. Selected Transformerless PV Inverters

Depending on the power ratings, transferring PV energy to an AC power grid has several possibilities [1], [7], [34]. It can be modular PV converters, which typically harvest the energy using DC-DC converters (maximum power point tracking) [36]-[38], while the string or central inverters can be directly connected to the grid. Since the grid-connected PV systems are still dominantly for residential applications [34], the single-phase transformerless PV inverter system is analyzed.

Figure 1 shows the most commonly used single-phase Full-Bridge (FB) PV inverter topology, where the modulation schemes have to be modified for a smaller leakage current (i_{CMV}). As it is shown in Figure 1, an *LCL*-filter is used for a better power quality. In some cases, a DC-DC converter is adopted to boost up the PV output voltage to an acceptable level for the PV inverters. Conventional modulation methods for the single-stage FB inverter topology include the bipolar modulation, the unipolar modulation, and the hybrid modulation. When considering the leakage current injection in transformerless applications, the bipolar modulation scheme is preferable [12], [22], which is chosen in this paper. Notably, optimizing the modulation patterns is an alternative to eliminate the leakage currents [19].

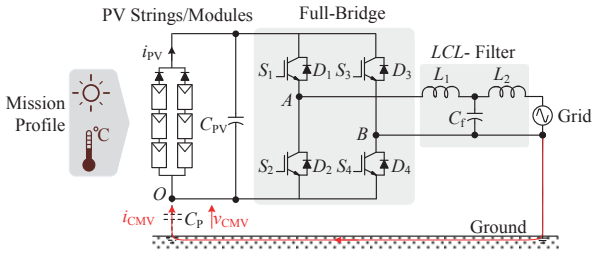

FIGURE 1: A single-phase single-stage grid-connected full-bridge PV inverter system with an *LCL*-filter, where v_{CMV} is the common mode voltage and C_P is the stray capacitor.

As mentioned early, transformerless structures are mostly derived from the FB topology by providing an AC path or a DC path using additional power switching devices. As a result, during the zero-voltage states, isolation between the PV modules and the grid is achieved, thus leading to a low leakage current injection. Figure 2 shows two examples of transformerless PV inverters derived from the single-phase FB topology. As it can be seen in Figure 2(a), the H6 inverter topology [13] has a DC path, which isolates the PV panels from the grid at zero-voltage states. In contrast, although the Highly Efficient and Reliable Inverter Concept (HERIC) [14] inverter has the same number of power switching devices as that of the H6 inverter, it provides an AC path to eliminate the leakage current injection.

It should be pointed out that there are also many other transformerless topologies reported in the literature in addition to the above two solutions [12], [39], [40]. For example, the Conergy Natural Point Clamped (NPC) transformerless PV inverter is based on the multi-level power converter technology [12], [20]. However, only the FB inverter with a bipolar modulation scheme (FB-Bipolar), the H6 inverter, and the HERIC inverter are assessed in terms of reliability.

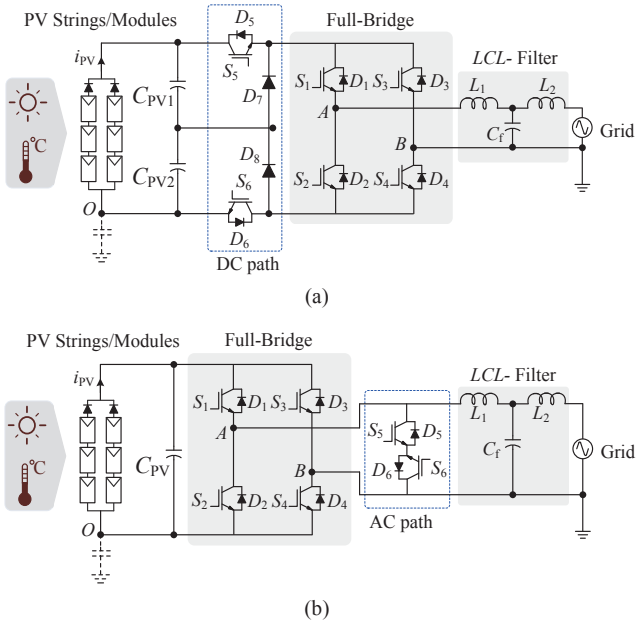

FIGURE 2: Examples of single-phase transformerless PV inverters derived from the single-phase full-bridge topology by adding extra power switching devices: (a) H6 inverter [13] and (b) HERIC inverter [14].

3. Mission Profile Translation to Thermal Loading

3.1. *Mission Profile for PV Systems*

A mission profile is normally referred as a simplified representation of relevant conditions under which the system is operating [28], [33]. As a result, for the grid-connected PV systems, the mission profile (i.e., solar irradiance and ambient temperature) is actually a reflection of the intermittent nature of the solar PV energy [35], and consequently it has an inherent relationship with the entire system performance, including the thermal loading performance. The mission profile can be a series of multi time-scales, e.g., a minute mission profile or a yearly mission profile, and it is usually taken as the input for the reliability analysis in the field of power electronics converters [30], [41]-[44], which is also focused on in this paper. Figure 3 shows the mission profile applied to the above three transformerless PV inverters.

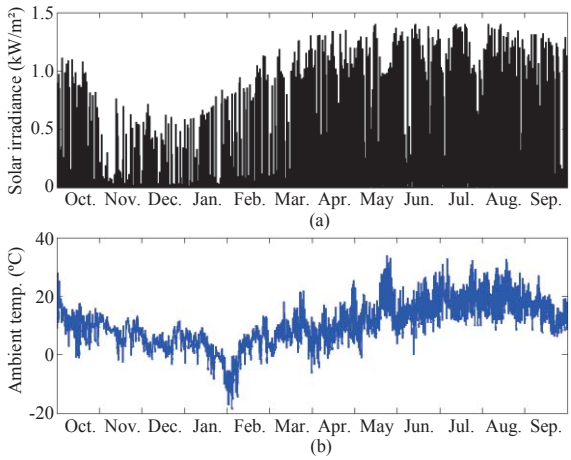

FIGURE 3: A yearly mission profile used for the selected transformerless PV inverters (1 sec/sample): (a) solar irradiance and (b) ambient temperature.

With more accumulative real-field experience and more advanced real-time monitoring technology, better mission profiles are available for a reasonable lifetime prediction. Hence, a mission profile based analysis approach should be able to analyze the performance at different time scales, as it is shown in Figure 4. It can be observed in Figure 4(a) that, for short-term mission profiles at the level of milliseconds to several seconds, the thermal loading profile can be directly and instantaneously obtained. In contrast, for long-term mission profiles within a range of a few minutes to several months, obtaining the instantaneous thermal loading will be very time-consuming or even impossible when the mission profile has a high data-sampling rate. Alternatively, the thermal loading profile can be obtained based on look-up tables [45], which are created in accordance to the short-term constant mission profiles, as it is shown in Figure 4(b).

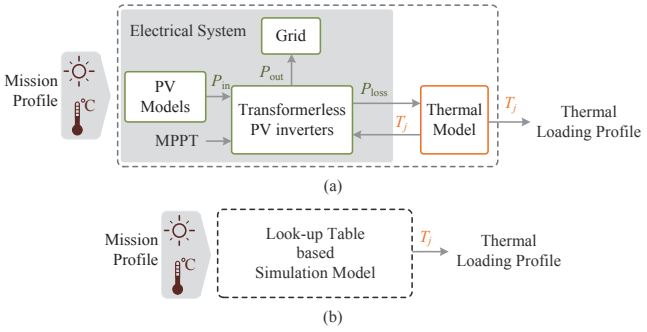

FIGURE 4: Approach of the mission profile translation to thermal loading at different time-scales (MPPT – Maximum Power Point Tracking, T_j – junction temperature of the power devices): (a) short-term mission profiles and (b) long-term mission profiles.

3.2. *Thermal Modelling of Power Switching Devices*

As it is shown in Figure 4, the translation from a mission profile to the corresponding thermal loading profile requires a thermal model which links the electrical performance (power losses, P_{loss}) and the thermal behavior (junction temperature, T_j). The coupled relationship is demonstrated in Figure 5 in a FB PV inverter system, which shows that the power losses on the switching devices will introduce a temperature rise due to the thermal impedance in the power switching devices. The thermal impedance can be modeled as a Foster model [45]-[49], as it is shown in Figure 6. Details of the thermal modelling of power semiconductors can be found in [48] and [49].

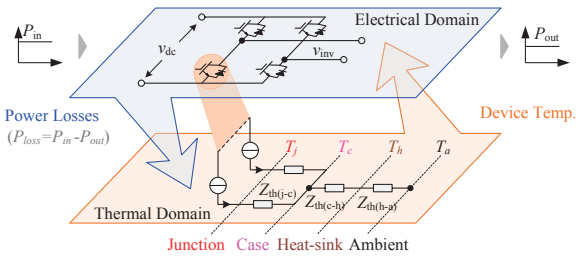

Notes: $Z_{th(j-c)}$- junction to case impedance
$Z_{th(c-h)}$- case to heat-sink impedance
$Z_{th(h-a)}$- heat-sink to ambient impedance

FIGURE 5: Coupled relationship between power losses and the junction temperature of the power switching devices.

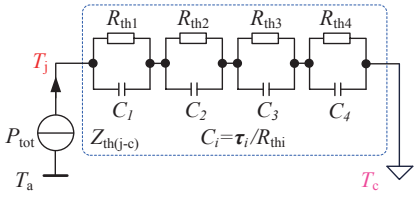

FIGURE 6: Foster model of the junction to case thermal impedance $Z_{th(j-c)}$ shown in Figure 5.

TABLE I: Thermal impedance parameters of a power switching devices from a leading manufacturer according to Figure 6.

Impedance		$Z_{th(j-c)}$			
i		1	2	3	4
IGBT	R_{thi} (K/W)	0.074	0.173	0.526	0.527
	τ_i (s)	0.0005	0.005	0.05	0.2
Diode	R_{thi} (K/W)	0.123	0.264	0.594	0.468
	τ_i (s)	0.0005	0.005	0.05	0.2

Typically, for such a model of the thermal impedance, the parameter data is provided in the datasheet. Table I shows the thermal parameters of the power switching device from a leading manufacturer used in the paper. Notably, all the devices are the same in the three transformerless PV inverters for comparison in terms of thermal loading, and thus the benchmarking results, indicating the critical components of transformerless PV inverters, could be a guidance to select appropriate power switching devices in such applications.

3.3. *Translated Thermal Loading to Lifetime*

Based on the thermal model, simulations have been carried out in PLECS [45] according to Figure 4, where the system parameters are shown in Table II. In order to create the look-up tables for long-term mission profiles, several constant operating conditions (e.g., solar irradiance: 0.8 kW/m^2, ambient temperature: 25 °C) have been simulated firstly, where a perturb-and-observe Maximum Power Point (MPP) tracking algorithm has been used [34]-[37]. Figure 7 exemplifies the simulation model for a full-bridge inverter system. A proportional resonant current controller has been adopted to control the grid current considering power quality requirements [2]. Using the look-up table model, the yearly mission profile (Figure 3) has been resampled (5 mins/sample) and translated into the thermal loading of the corresponding power switching devices, as it is presented in Figure 8.

TABLE II: System Parameters for Single-Phase Transformerless Grid-Connected PV Systems.

Parameter	Symbol	Value	Unit
Grid voltage	$v_{g,RMS}$	230	V
Grid frequency	f_g	50	Hz
LCL filter	L_1	3.6	mH
	C_f	2.35	μF
	L_2	4	mH
Damping resistor	R_d	10	Ω
Switching frequency	f_s	10	kHz
Parameters of PV Strings (3 strings, 15 panels for each string) at 25 °C and 1 kW/m^2			
Power at MPP	P_{MPP}	2.99	kW
Voltage at MPP	V_{MPP}	405	V
Current at MPP	I_{MPP}	7.38	A

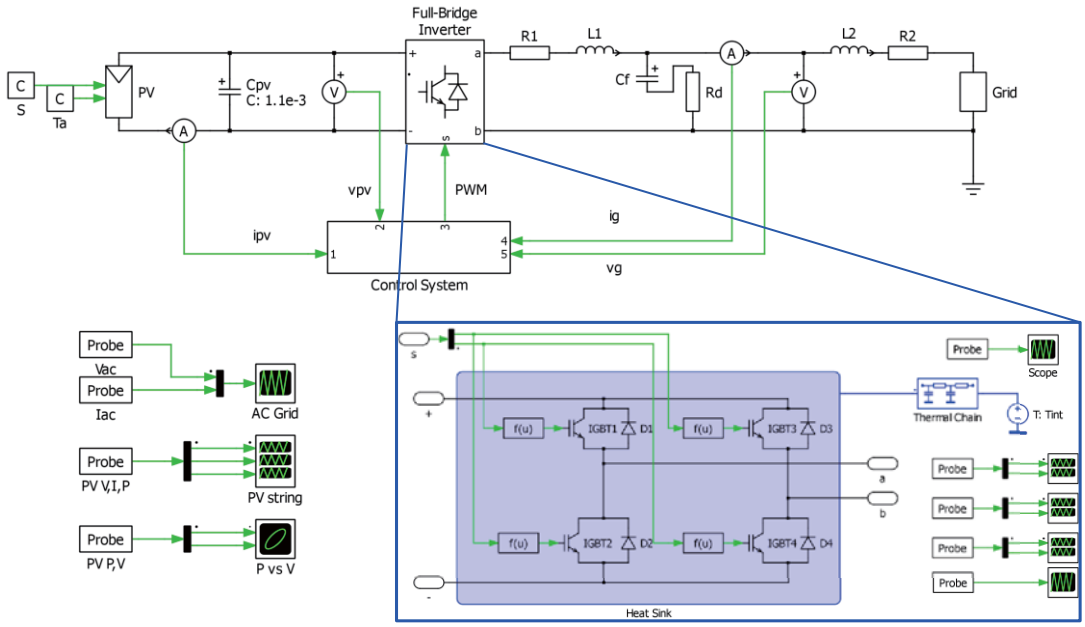

FIGURE 7. Simulation model of a single-phase full-bridge PV inverter system in PLECS.

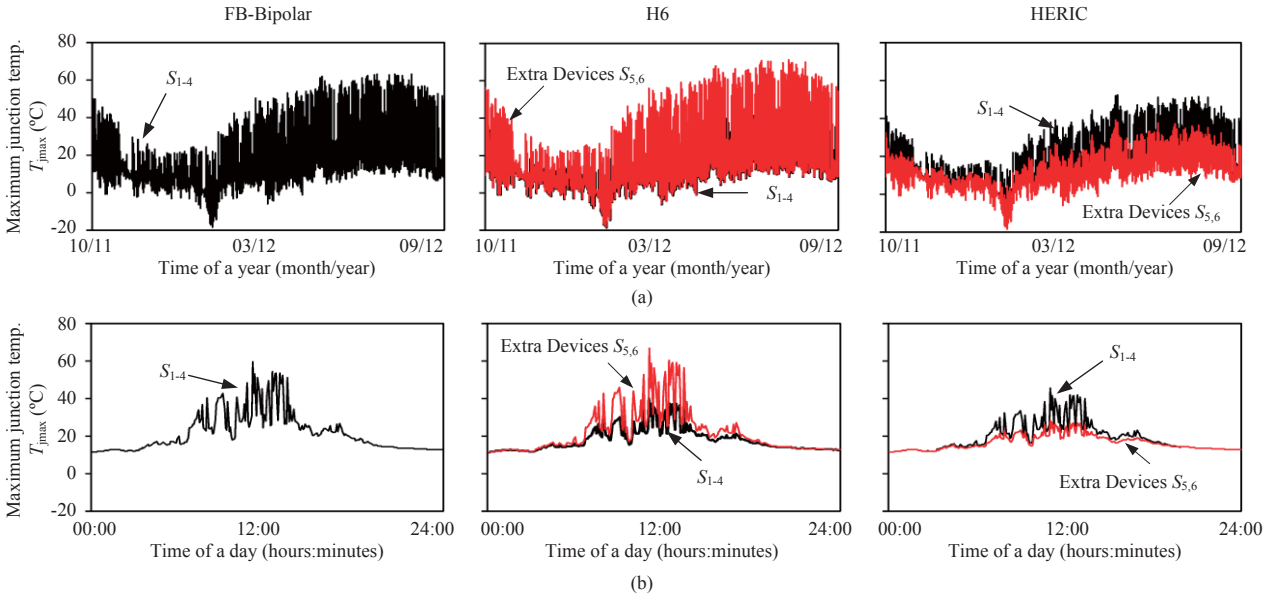

FIGURE 8: Translated thermal loading (maximum junction temperature, T_{jmax}) of the power switching devices of the three different transformerless grid-connected PV inverters under a yearly mission profile shown in Figure 3: (a) the yearly long-term thermal loading and (b) details of the maximum junction temperature of the power switching devices in a cloudy day of the year.

Although the transformerless PV inverters (both the H6 and the HERIC) can maintain a higher efficiency as reported in the literature in contrast to the FB-Bipolar inverter, the thermal loading on those switching devices is unequal, as it can be seen in Figure 8. Specifically, the maximum junction temperature of the extra devices in a H6 inverter is the highest, indicating high power losses, since they are switched at a high frequency. However, this is not the case for the HERIC inverter, where only one of the extra switching devices is switched at the grid frequency during a half cycle. Therefore, the power losses are lower, and thus the thermal loading as it is shown in Figure 8. From the above qualitative analysis, it is implied that much attention has to be paid on the extra switching devices in transformerless PV inverters. Especially for the H6 inverter, power switching devices with lower conduction losses and higher rated maximum junction temperature are desirable, while the total cost has to be taken into considerations as well.

When the thermal loading profile appearing in the power switching devices is available, a quantitative prediction of the device lifetime under the mission profile is enabled by a rain-flow counting algorithm [43], [44]. The rain-flow counting algorithm is a quantitative representation of the thermal loading, which extracts the temperature information in details in

terms of the mean junction temperature T_{jm}, temperature cycle amplitude T_j, cycle period t_{on}, number of cycles n, and etc.. Then, the extracted temperature information can be used for the lifetime prediction according to a specific lifetime model. For example, a lifetime model of power switching devices is introduced in [50] and it can be expressed as,

$$N_f = A\Delta T_j^{\alpha}\left(ar\right)^{\beta_1 \Delta T_j + \beta_0}\left(\frac{C+\left(t_{on}\right)^{\gamma}}{C+1}\right)\exp\left(\frac{E_a}{k_B T_{jm}}\right) f_d \tag{1}$$

where N_f is the number of cycles to fail, f_d is the diode effect, ar is the bond-wire aspect ratio, k_B is the Boltzmann constant, E_a is the activation energy, and A, α, β_0, β_1, γ, C are the lifetime model parameters, as it is shown in Table III. The lifetime model also implies that the junction temperature has a significant impact on the number of cycles to fail, i.e. the reliability of the power switching devices.

TABLE III: Parameters of the Lifetime Model for a Power Devices [50].

Parameter	Value	Unit	Experimental Condition
A	3.4368×10^{14}	-	
α	-4.923	-	$64\ \text{K} \le \Delta T_j \le 113\ \text{K}$
β_0	1.942	-	$0.19 \le ar \le 0.42$
β_1	-9.012×10^{-3}	-	
C	1.434	-	$0.07\ \text{s} \le t_{on} \le 63\ \text{s}$
γ	-1.208	-	
f_d	0.6204	-	
E_a	0.06606	eV	$32.5\ °\text{C} \le T_{jm} \le 122\ °\text{C}$
k_B	8.6173324×10^{-5}	eV/K	

According to the Miner's rule [25], [44], [50], the Life Consumption LC - the damage due to the thermal stress is the linearly accumulative damage from different thermal cycles. The LC can then be expressed as,

$$LC = \sum_i \frac{n_i}{N_{fi}} \tag{2}$$

in which n_i is the number of cycles at the stress ΔT_{ji} extracted by the rain-flow counting algorithm, and N_{fi} is the number of cycles to fail based on (1). Subsequently, the lifetime of the power switching devices can be given as,

$$L_P = \frac{t_{MP}}{LC} \tag{3}$$

with L_P being the predicted lifetime, and t_{MP} being the mission profile period (e.g., a year).

Using the above reliability analysis procedure, the lifetime of the power switching devices in the transformerless PV inverters can then be estimated as long as a mission profile and a lifetime model of high confidence are available. Figure 9 summarizes the mission profile based analysis approach, which can also be used in other power electronics converters, e.g., wind turbine converters, where the mission profiles are available.

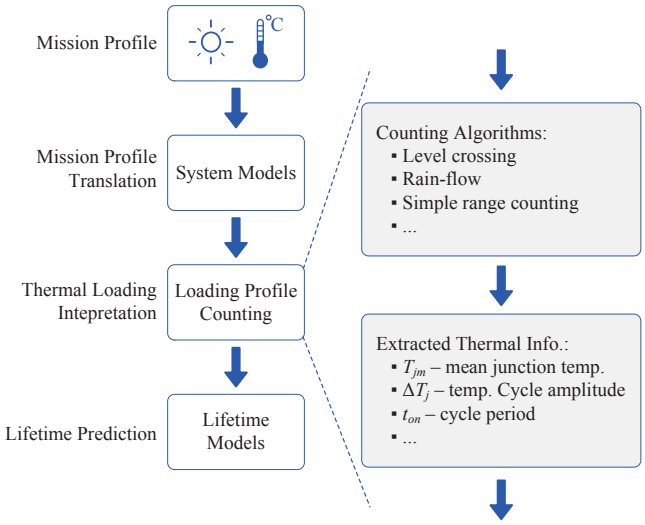

FIGURE 9: Flow-chart of the mission profile based reliability analysis approach for transformerless PV inverters.

4. Reliability Assessment

According to Figure 9, the lifetime of the power switching devices in the three transformerless PV inverters under the yearly mission profile shown in Figure 3 can be obtained and evaluated. In order to benchmark the reliability quantitatively, the thermal loading profiles have to be interpreted first according to (1) and Figure 9. A rain-flow counting algorithm has been adopted, and the results are presented in Figure 10. It can be observed in Figure 10 that the additional devices of the H6 inverter (i.e., S_5 and S_6) have a larger number of cycles compared to the other power switching devices of this topology ($S_{1\sim4}$). This indicates that the extra devices to realize an elimination of the leakage currents become the most critical components of the H6 inverter according to (2) and (3). As a consequence, more reliable power devices are preferable as the extra devices when designing an H6 based transformerless PV system. In the case of the HERIC inverter based transformerless PV systems, the extra devices have a smaller number of cycles compared to that of the H6 inverter. Moreover, the number of cycles of the other power switching devices of the HERC inverter is even smaller than that of the FB-Bipolar inverter under the same mission profile. This means that the thermal stress on the power switching devices of the HERIC inverter is the lowest, and thus the highest reliability under the same mission profile, while also maintaining a higher efficiency as it is reported in [12], [14]. The discussion is in agreement with the analysis presented in § 3.3 based on the translated thermal loading profiles.

It should be noted that the life consumption and thus the lifetime of the power switching devices according to (2) and (3) can quantitatively be obtained on condition that the lifetime model of (1) and also the parameters given in Table III are at a high confident level. However, those parameters are extracted under specific conditions (e.g., $0.07\ \text{s} \le t_{on} \le 63\ \text{s}$) for the power switching devices introduced in [50]. Therefore, quantitative prediction errors will be inevitable. In order

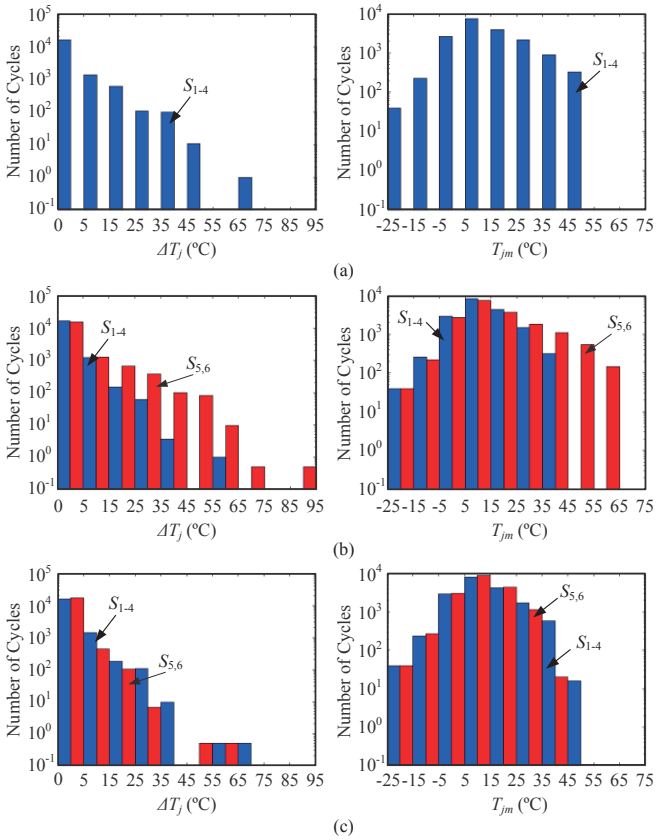

FIGURE 10: Rain-flowing counting results (number of cycles distributions at the cycle amplitude ΔT_j and the mean junction temperature T_{jm}) of the thermal loading profiles shown in Figure 8: (a) FB-Bipolar inverter, (b) H6 inverter, and (c) HERIC inverter.

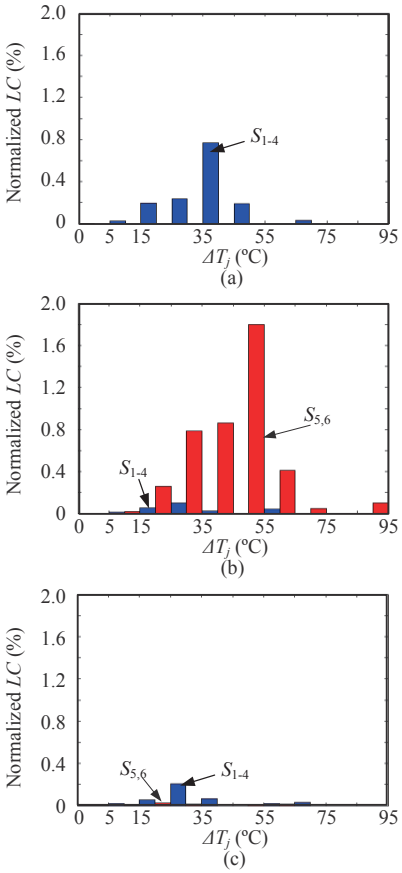

FIGURE 11: Normalized life consumption (lifetime comparison) of the three transformerless PV inverters under the same mission profile: (a) FB-Bipolar inverter, (b) H6 inverter, and (c) HERIC inverter.

to reduce the parameter dependency and also the reliability model dependency, the life consumption given in (2) is normalized, and substituting (1) yields,

$$\overline{LC} = \frac{LC}{LC_b} = \frac{\sum_i \frac{n_i}{\left(\Delta T_{ji}\right)^{\alpha}\left(ar\right)^{\beta_1 \Delta T_{ji}}\left[C+\left(t_{oni}\right)^{\gamma}\right]e^{E_a/\left(k_B T_{jmi}\right)}}}{\sum_l \frac{n_l}{\left(\Delta T'_{jl}\right)^{\alpha}\left(ar\right)^{\beta_1 \Delta T'_{jl}}\left[C+\left(t'_{onl}\right)^{\gamma}\right]e^{E_a/\left(k_B T'_{jml}\right)}}} \tag{4}$$

where $\overline{LC}$ is the normalized life consumption, and LC_b is the base LC for normalization. For example, LC_b can be chosen as the life consumption of the power switching devices of the FB-Bipolar inverter under the same mission profile. Then, the predicted lifetime can be expressed as,

$$L_p = \frac{1}{\overline{LC}} L'_p \tag{5}$$

in which L'_p is the predicted lifetime of the base system used for normalization.

Figure 11 shows the normalized life consumption of the three transformerless PV inverters according to (4) and the counting results enabled by a rain-flow algorithm. The life consumption of the power switching devices of the FB-Bipolar (i.e., $S_{1\sim4}$) is selected as the base life consumption for normalization in Figure 11. It can be seen in Figure 11 that the extra power switching devices of the H6 inverter consume much more life compared to the other devices and also those of the HERIC inverter. It implies that the degradation of the additional devices of the H6 inverter happens much faster, and then the entire H6 system may fail to operate earlier than the other two transformerless PV inverters. This comparison further confirms that the HERIC inverter would be the most promising solution in terms of reliability.

In addition, by comparing the rain-flow counting results shown in Figure 10 with the normalized life consumption shown in Figure 11, one interesting conclusion can be drawn is that, although there are a few cycles of a large temperature cycling amplitude (e.g., ten cycles of 55 °C to 65 °C for the extra devices $S_{5,6}$ of the H6 inverter), they do contribute much more damage (e.g., 0.4% in Figure 11(b)) when the lifetime model of (1) is adopted. Large cycling amplitude are mainly induced by the mission profile, which confirms that the mission profile effect has to be taken into account in a reliability-oriented design of power electronics converters. In a word,

the reliability assessment in this paper reveals that much attention has to be put on the thermal design of the critical components in an entire PV inverter in order to reduce the cost of energy.

5. Conclusions

In this paper, a qualitative reliability assessment of three selected single-phase transformerless PV inverters has been carried out in accordance to a mission profile based reliability analysis approach. A real-field yearly mission profile has been applied to the selected transformerless candidates for the reliability assessment. The comparison results have revealed that, although minimizing leakage currents as well as maintaining a satisfactory efficiency has been targeted by those inverters, the extra devices that are used for disconnection of the PV panels or the PV inverters might be heated up during operation. The high thermal loading will further induce failures of the power switching devices, being a big challenge to the entire system reliability. As a consequence, many efforts should be devoted to a reliability-oriented design of the critical components in a PV inverter, and thus a reduced cost of energy can be achieved.

References

[1] F. Blaabjerg, K. Ma, and Y. Yang, "Power electronics - The key technology for Renewable Energy Systems," in *Proc. of EVER*, pp. 1-11, 25-27 Mar. 2014.

[2] F. Blaabjerg, R. Teodorescu, M. Liserre, and A.V. Timbus, "Overview of control and grid synchronization for distributed power generation systems," *IEEE Trans. Ind. Electron.*, vol. 53, no. 5, pp. 1398-1409, Oct. 2006.

[3] J.M. Carrasco, L.G. Franquelo, J.T. Bialasiewicz, E. Galvan, R.C.P. Guisado, Ma.A.M. Prats, J.I. Leon, and N. Moreno-Alfonso, "Power-electronic systems for the grid integration of renewable energy sources: a survey," *IEEE Trans. Ind. Electron.*, vol. 53, no. 4, pp. 1002-1016, June 2006.

[4] J.D. van Wyk, and F.C. Lee, "On a future for power electronics," *IEEE J. Emerging and Selected Topics in Power Electron.*, vol. 1, no. 2, pp. 59-72, June 2013.

[5] A. Golnas, "PV system reliability: an operator's perspective," *IEEE J. Photovoltaics*, vol. 3, no. 1, pp. 416-421, Jan. 2013.

[6] A. Ristow, M. Begovic, A. Pregelj, and A. Rohatgi, "Development of a methodology for improving photovoltaic inverter reliability," *IEEE Trans. Ind. Electron.*, vol. 55, no. 7, pp. 2581-2592, July 2008.

[7] E. Romero-Cadaval, G. Spagnuolo, L. Garcia Franquelo, C.A. Ramos-Paja, T. Suntio, and W.M. Xiao, "Grid-connected photovoltaic generation plants: components and operation," *IEEE Ind. Electron. Mag.*, vol. 7, no. 3, pp. 6-20, Sept. 2013.

[8] REN21, "Renewables 2014 Global Status Report," Tech. Rep., pp. 1-216, 2014. Available Online: www.ren21.net.

[9] M. Liserre, T. Sauter, and J.Y. Hung, "Future energy systems: integrating renewable energy sources into the smart power grid through industrial electronics," *IEEE Ind. Electron. Mag.*, vol. 4, no. 1, pp. 18-37, Mar. 2010.

[10] C.-L. Shen and S.-H. Yang, "Multi-Input Converter with MPPT Feature for Wind-PV Power Generation System," *International Journal of Photoenergy*, vol. 2013, Article ID 129254, 13 pages, 2013. doi:10.1155/2013/129254.

[11] F. Blaabjerg and K. Ma, "Future on power electronics for wind turbine systems," *IEEE J. Emerging and Selected Topics in Power Electron.,* vol. 1, no. 3, pp. 139-152, Sept. 2013.

[12] R. Teodorescu, M. Liserre, and P. Rodriguez. *Grid Converters for Photovoltaic and Wind Power Systems*. Wiley & IEEE. 2011.

[13] R. Gonzalez, J. Lopez, P. Sanchis, and L. Marroyo, "Transformerless inverter for single-phase photovoltaic systems," *IEEE Trans. Power Electron.*, vol. 22, no. 2, pp. 693-697, Mar. 2007.

[14] H. Schmidt, C. Siedle, and J. Ketterer, "DC/AC converter to convert direct electric voltage into alternating voltage or into alternating current." U.S. Patent 7046534, Issued May 16, 2006.

[15] T. Kerekes, M. Liserre, R. Teodorescu, C. Klumpner, and M. Sumner, "Evaluation of three-phase transformerless photovoltaic inverter topologies," *IEEE Trans. Power Electron.*, vol. 24, no. 9, pp. 2202-2211, Sept. 2009.

[16] R. Gonzalez, E. Gubia, J. Lopez, and L. Marroyo, "Transformerless single-phase multilevel-based photovoltaic inverter," *IEEE Trans. Ind. Electron.*, vol. 55, no. 7, pp. 2694-2702, July 2008.

[17] I. Patrao, E. Figueres, F. González-Espín, G. Garcerá, "Transformerless topologies for grid-connected single-phase photovoltaic inverters," *Renewable and Sustainable Energy Reviews*, vol. 15, no. 7, pp. 3423-3431, Sept. 2011.

[18] Advanced Energy, "What's ahead for PV inverter technology?" *greentechsolar*, Available Online: www.greentechmedia.com/, 23 Jul. 2014.

[19] N. Achilladelis, E. Koutroulis, and F. Blaabjerg, "Optimized pulse width modulation for transformerless active-NPC inverters," in *Proc. of EPE'14-ECCE Europe*, pp. 1-10, 26-28 Aug. 2014.

[20] S. Saridakis, E. Koutroulis, and F. Blaabjerg, "Optimal design of modern transformerless PV inverter topologies," *IEEE Trans. Energy Convers.*, vol. 28, no. 2, pp. 394-404, Jun. 2013.

[21] I. Patrao, E. Figueres, F. González-Espín, and G. Garcerá. "Transformerless topologies for grid-connected single-phase photovoltaic inverters," *Renewable and Sustainable Energy Reviews*, vol. 15, no. 7, pp. 3423-3431, 2011.

[22] Y. Yang, H. Wang, F. Blaabjerg, and K. Ma. "Mission profile based multi-disciplinary analysis of power modules in single-phase transformerless photovoltaic inverters," in *Proc. of EPE*, pp. 1-10, Sept. 2013.

[23] S.E. De León-Aldaco, H. Calleja, F. Chan, and H.R. Jiménez-Grajales, "Effect of the mission profile on the reliability of a power converter aimed at photovoltaic applications—a case study," *IEEE Trans. Power Electron.*, vol. 28, no. 6, pp. 2998-3007, Jun. 2013.

[24] H. Wang, M. Liserre, and F. Blaabjerg, "Toward reliable power electronics: challenges, design tools, and opportunities," *IEEE Ind. Electron. Mag.*, vol. 7, no. 2, pp. 17-26, June 2013.

[25] H. Huang and P.A. Mawby, "A lifetime estimation technique for voltage source inverters," *IEEE Trans. Power Electron.*, vol. 28, no. 8, pp. 4113-4119, Aug. 2013.

[26] P. McCluskey, "Reliability of power electronics under thermal loading," in *Proc. of CIPS*, pp. 1-8, 6-8 Mar. 2012.

[27] H. Lu, C. Bailey, and C. Yin, "Design for reliability of power electronics modules," *Microelectronics Reliability*, vol. 49, no. 9–11, pp. 1250-1255, Sept.–Nov. 2009.

[28] M. Ciappa, "Lifetime prediction on the base of mission profiles," *Microelectronics Reliability*, vol. 45, no. 9–11, pp. 1293-1298, Sept.–Nov. 2005.

[29] F. Chan and H. Calleja, "Reliability estimation of three single-phase topologies in grid-connected PV systems," *IEEE Trans. Ind. Electron.*, vol. 58, no. 7, pp. 2683-2689, July 2011.

[30] K. Ma, M. Liserre, F. Blaabjerg, and T. Kerekes, "Thermal loading and lifetime estimation for power device considering mission profiles in wind power converter," *IEEE Trans. Power Electron.*, vol. 30, no. 2, pp. 590-602, Feb. 2015.

[31] S. Harb and R.S. Balog, "Reliability of candidate photovoltaic module-integrated-inverter (PV-MII) topologies- A usage model approach," *IEEE Trans. Power Electron.*, vol. 28, no. 6, pp. 3019-3027, Jun. 2013.

[32] P. Zhang, Y. Wang, W. Xiao, and W. Li, "Reliability evaluation of grid-connected photovoltaic power systems," *IEEE Trans. Sustain. Energy*, vol. 3, no. 3, pp. 379-389, Jul. 2012.

[33] S.E. De León-Aldaco, H. Calleja, and J. Aguayo, "Reliability and mission profiles of photovoltaic systems: a FIDES approach," *IEEE Trans. Power Electron.*, vol. 30, no. 5, pp. 2578 - 2586, May 2015.

[34] S.B. Kjaer, J.K. Pedersen, and F. Blaabjerg, "A review of single-phase grid-connected inverters for photovoltaic modules," *IEEE Trans. Ind. Appl.*, vol. 41, no .5, pp. 1292-1306, Sept.-Oct. 2005.

[35] A. Hajiah, T. Khatib, K. Sopian, and M. Sebzali, "Performance of grid-connected photovoltaic system in two sites in Kuwait," *International Journal of Photoenergy*, vol. 2012, Article ID 178175, 7 pages, 2012. doi:10.1155/2012/178175.

[36] H. Li, J. Peng, W. Liu, Z. Huang, and K.-C. Lin, "A newton-based extreme seeking MPPT method for photovoltaic systems with stochastic perturbations," *International Journal of Photoenergy*, vol. 2014, Article ID 938526, 13 pages, 2014. doi:10.1155/2014/938526.

[37] D. Sera, L. Mathe, T. Kerekes, S.V. Spataru, and R. Teodorescu, "On the perturb-and-observe and incremental conductance MPPT methods for PV systems," *IEEE J. Photovoltaics*, vol. 3, no. 3, pp. 1070-1078, Jul. 2013.

[38] M. Abdulkadir, A. H. M. Yatim, and S. T. Yusuf, "An Improved PSO-Based MPPT Control Strategy for Photovoltaic Systems," *International Journal of Photoenergy*, vol. 2014, Article ID 818232, 11 pages, 2014. doi:10.1155/2014/818232.

[39] R. Gonzalez, E. Gubia, J. Lopez, and L. Marroyo, "Transformerless single-phase multilevel-based photovoltaic inverter," *IEEE Trans. Ind. Electron.*, vol. 55, no. 7, pp. 2694-2702, Jul. 2008.

[40] Y. Zhou and H. Li, "Analysis and suppression of leakage current in cascaded-multilevel-inverter-based PV systems," *IEEE Trans. Power Electron.*, vol. 29, no. 10, pp. 5265-5277, Oct. 2014.

[41] M. Musallam, C. Yin, C. Bailey, and M. Johnson, "Mission profile based reliability design and real-time life consumption estimation in power electronics," *IEEE Trans. Power Electron.*, vol. 30, no. 5, pp. 2601-2613, May 2015.

[42] Y. Yang, H. Wang, F. Blaabjerg, and T. Kerekes, "A hybrid power control concept for PV inverters with reduced thermal loading," *IEEE Trans. Power Electron.*, vol. 29, no. 12, pp. 6271-6275, Dec. 2014.

[43] A.T. Bryant, P.A. Mawby, P.R. Palmer, E. Santi, and J.L. Hudgins, "Exploration of power device reliability using compact device models and fast electrothermal simulation," *IEEE Trans. Ind. Appl.*, vol. 44, no. 3, pp. 894-903, May-Jun. 2008.

[44] M. Musallam and C.M.; Johnson, "An efficient implementation of the rainflow counting algorithm for life consumption estimation," *IEEE Trans. Reliability*, vol. 61, no. 4, pp. 978-986, Dec. 2012.

[45] Plexim Gmbh., "PLECS – The simulation platform for power electronics systems," *Workshop Documentation*, vol. 1, Aalborg, Oct. 2014.

[46] I.F. Kovačević, U. Drofenik, and J.W. Kolar, "New physical model for lifetime estimation of power modules," in *Proc. of IPEC*, pp. 2106-2114, June 2010.

[47] C. Busca, R. Teodorescu, F. Blaabjerg, S. Munk-Nielsen, L. Helle, T. Abeyasekera, and P. Rodriguez, "An overview of the reliability prediction related aspects of high power IGBTs in wind power applications," *Microelectronics Reliability*, vol. 51, no. 9–11, pp. 1903-1907, Sept.–Nov. 2011.

[48] ABB, "Application Note – Applying IGBTs," [Online]. Available: http://www.abb.com, 13 Jan. 2014.

[49] A. Volke and M. Hornkamp. *IGBT Modules – Technologies, Driver and Application*. Infineon Technologies AG, Munich, 2012.

[50] U. Scheuermann, "Reliability of advanced power modules for extended maximum junction temperatures," *Bodo's Power Systems*, pp. 26-30, Sept. 2014.